First International Symposium on Marine Propulsors
smp'09, Trondheim, Norway, June 2009

Numerical and Experimental Investigation into Cavitation of Propellers Having Blades Designed by Various Load Distributions near the Blade Tips

Shosaburo Yamasaki[1], Akinori Okazaki[1], Nobuhiro Hasuike[1], Yasutaka Kawanami[2], Yoshitaka Ukon[2]

[1]Nakashima Propeller Co.,Ltd., Okayama, Japan
[2] National Maritime Research Institute (NMRI), Mitaka, Tokyo, Japan

ABSTRACT

This paper discusses the effectiveness of cavitation control by tip load distribution as a propeller design parameter and presents the results of systematic experiments and numerical computations to develop practical design tools for high-performance marine propeller.

A recent propeller design showed that a tip loaded propeller offered better results against cavitation erosion than a tip unloaded one. In order to study the effect of tip load distribution on the cavitation characteristics in detail, seven propellers were designed with systematically varied load distributions near the blade tip. Two four-bladed propeller models were manufactured. Their each individual blade had the different tip load distribution designed systematically.

On these models, the cavitation observation by a high-speed video camera and the pressure fluctuation measurement were carried out. The more heavily tip loaded blade demonstrated the better cavitation performance than other loaded blades on both erosion and pressure fluctuations.

To validate existing numerical tools, cavitation pattern was numerically simulated by a classical lifting surface code and a Reynolds-Averaged Navier-Stokes solver. Both methods are found to be useful for predicting the effect of tip load distribution on the cavitation behavior on the propeller blades working in the non-uniform flow.

Keywords

Propeller Design, Tip Loaded Propeller, Cavitation Erosion, Pressure Fluctuations, Numerical Simulation

1 INTRODUCTION

The load distribution of propeller blades especially near the tip plays an important role not only on propeller efficiency but also on cavitation performance, e.g., (Johnsson 1981), (Holden 1983). It is well known that highly efficient wake adapted propellers for large size merchant ships can be designed by applying for tip loaded propellers with taking the hull wake distribution into account, e.g., (Lerbs 1952), (Eckhardt & Morgan 1955). On the other hand, in the modern practical design of marine propellers, tip unloaded distributions are often applied to a number of propellers to reduce cavitation related problems, such as hull vibration and erosion.

Recently the authors have found that tip loaded propellers offered better results against cavitation erosion in several model tests on small blade area propellers aiming at increase in the efficiency. In this paper, seven types of propellers were designed with the tip load distribution varied systematically to examine the reason why the tip loaded propeller is more effective against cavitation problems than the commonly used tip unloaded one and to find the design criteria on the prevention against cavitation erosion.

In order to investigate the relation between the tip load distribution and the cavitation performance with high cost effectiveness, two types of four-bladed propeller models were manufactured whose individual blades have different tip load distributions. These special propeller models are very effective to perform cavitation tests with less experimental uncertainty due to water quality in a cavitation tunnel. This experimental technique was applied for cavitation tests, e.g., (Takahashi 1959), (Ukon 1981).

In cavitation erosion tests, careful and detailed observation on the cavitation behavior around the propeller blades is needed with advanced photographical techniques, when they are working in a non-uniform wake. A high-speed video camera can be effectively used in the systematic of cavitation experiments to examine the cavitation behavior and to analyze the video images taken during the growing and collapsing process of the sheet cavity on these propellers.

In order to design high performance propellers without any cavitation problems, numerical simulation tools are

needed to predict cavitation pattern on the propeller blades reliably. As to numerical simulation methods of cavitation pattern on unsteady propellers, numerous methods have been proposed. In this paper, a classical Lifting Surface Theory (LST in short), e.g., (Yamasaki 1981) and a RANS solver, e.g., (Hasuike et al 2006), (Hasuike & Yamasaki 2006) were employed for cavitation simulation.

Based on the experimental and numerical simulation results, the authors discuss the relationship between the blade load distribution near the tip and cavitation erosion, new findings about collapsing behavior of cavitation and the validity of cavitation simulation by the LST and the RANS codes.

2 DESIGN OF PROPELLER WITH SYSTEMATICALLY VARIED TIP LOAD DISTRIBUTION

2.1 Propeller Design

In order to study the influence of tip load distribution on cavitation problems in detail, a propeller (PNo.0) for a containership was selected as a prototype and designed by the conventional standard to determine the blade area, e.g., (Yamasaki & Okazaki 2005).

Seven types of propellers were designed by keeping the thrust coefficient K_T 0.15 for the design point and by systematically varying the blade tip load from heavily loaded to lightly loaded distributions using the LST for a container ship. Table 1 shows the propeller design condition and Figure 1 shows the hull wake pattern of the containership. Table 2 gives the main dimensions of seven designed propellers indicated from PNo.1 to PNo.7 and the prototype (PNo.0). The larger the propeller number, the heavier the blade load near the tip, i.e. the tip load of PNo.7 is the heaviest among seven propellers. Figure 2 shows the comparison of the radial pitch distribution among these propellers.

The main dimensions, the number of blades, the diameter, the skew angle and others of seven designed propellers for the present study are the same as those of PNo.0. On the other hand, the blade area ratio is 20% smaller than that of PNo.0 aiming at higher propeller efficiency. These propellers have the tip slightly raked to the pressure side. The blade load distribution near the tip of PNo.3 is similar to that of PNo.0.

Table 1 Propeller design condition

Kind of ship		Container
BHP (MCR) (for strength)	kW	32,940
N (MCR) (for strength)	rpm	100
BHP (CSO) (for pitch)	kW	28,000
N (CSO) (for pitch)	rpm	94.7
RPM margin	%	4.5
Vs (CSO)	knot	26.6
1-ws (CSO)		0.8
Immersion	m	7.5

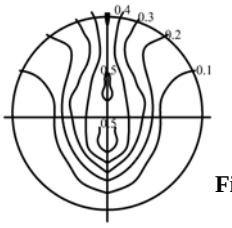

Figure 1 Wake pattern

Table 2 Propeller main dimension

PNo.		0	1	2	3
MPNo.		0	1-D	1-C	1-B
Number of Blades		4			
Diameter	m	8.2			
Expanded Area Ratio		0.65	0.52		
Pitch Ratio (0.7R)		1.124	1.105	1.077	1.051
Skew Angle	deg.	30			
PNo.		4	5	6	7
MPNo.		1-A,2-A	2-B	2-C	2-D
Number of Blades		4			
Diameter	m	8.2			
Expanded Area Ratio		0.52			
Pitch Ratio (0.7R)		1.026	1.002	0.979	0.957
Skew Angle	deg.	30			

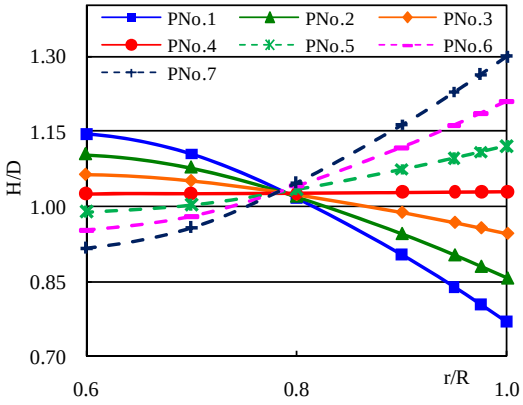

Figure 2 Pitch distribution

2.2 Calculation of Propeller Characteristics

Figure 3 and Table 3 show the circulation distribution and the open characteristics of the propellers working in the averaged wake of this containership at the design condition. They are estimated by the LST, e.g., (Yamasaki 1981). All of the circulation distribution curves of seven propellers cross at the location slightly below 0.8R due to the design constraint to generate the same thrust under the various blade tip loadings. The heavier the blade load near the tip becomes, the larger the circulation near the tip and in contrast the smaller that near the boss become.

From the comparison of the computed propeller open efficiency, the efficiencies of PNo.3 and 4 are the highest. On the other hand, the increase or the decrease in the blade load near the tip reduces the propeller efficiency. For example, the efficiency of PNo.7 with the heaviest tip load is decreased by 4.1% against that of PNo.3 and 4.

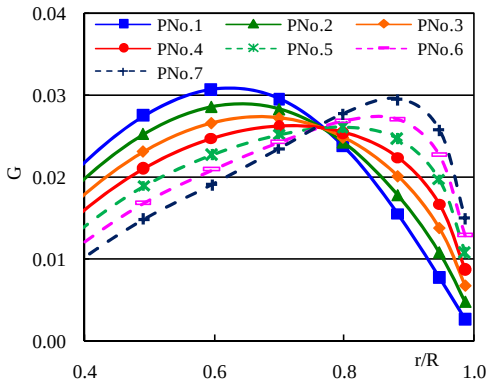

Figure 3 Circulation distribution

Table 3 Estimated propeller open characteristics

PNo.	0	1	2	3	4	5	6	7
J	0.810							
K_T	0.150							
$10K_Q$	0.267	0.266	0.263	0.261	0.261	0.263	0.267	0.272
ηo	0.725	0.726	0.736	0.741	0.741	0.735	0.725	0.710

3 MODEL TEST OF PROPELLERS HAVING VARIOUS LOAD DISTRIBUTIONS NEAR THE BLADE TIPS

As mentioned above, two types of four-bladed propeller models were tested, whose blades have the different various tip load distributions to carry out the model test effectively. Each blade of the four-bladed propeller models can be specified by single alphabetical character after the propeller number, namely MP1-.A, B, C, D and MP2-A, B, C, D. corresponding to PNo.4, 3, 2, 1 and PNo.4, 5, 6, 7 respectively. The blades A of both propeller models are the same geometrical shape as a common blade.

By using the present models in the cavitation tests, cavitation patterns on four kinds of blades can be observed during one test run and evaluated cavitation characteristics on each blade easily. On the other hand, small influence on cavitation due to the interference from the neighboring different blades cannot be avoided, not as that of the prototype propeller model (MPNo.0) with all the blades of the same shape. Figure 4 shows the photographs of propeller models described in this paper.

The cavitation experiments on these models were carried out in the cavitation tunnel of the IHI Corporation R&D Project Center using a video camera with stroboscopic light source and a high-speed video camera with metal halide lamps. The pressure fluctuation measurements were performed on the flat plate which located just above the propeller model. The wake pattern as shown in Figure 1 was reconstructed by a wire mesh screen.

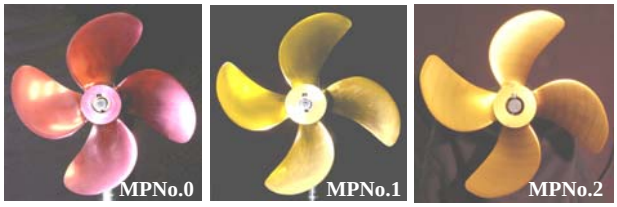

Figure 4 Propeller models

3.1 Cavitation Observation

In order to take pictures of the cavitation behavior on the blades by a high speed video camera (Vision Research, Inc, Phantom V7.3) clearly, a prism made of acrylic resin was set up at the observation window and the four halide lighting system was used to increase the intensity of the light source. The capturing frame speed of this camera was set to 6,000 ~ 10,000 frames per sec. Since the propeller rotational speed was about 25 rps, the video was recorded by 240 ~ 400 frames per revolution corresponding to about 0.7 ~ 1 frame per degree.

The thrust coefficient K_T of the propeller and the cavitation number σ_n for the high-speed video observation was set to 0.161 and 1.7 respectively. Figure 5 to 8 are the series of representative flames of cavitation taken by the high-speed video camera. Figure 5 and 6 indicate the process from the cavitation inception to the collapse of sheet cavity on MP1-A and D. Figure 7 and 8 indicate the cavitation patterns in each stage of cavity growth, development and decline on MP1-B and C, and MP2-B, C and D. From the analysis from these pictures and the animations of a high-speed video camera, the cavitation behaviors on each blade can be summarized as follows.

(1) The extent of blade surface cavitation on MP1-D (the most lightly loaded propeller) was the largest and the collapsing time of the sheet cavity was the shortest. When the size of the sheet cavitation on the blade reached the maximum, it extended from around 0.5R to the tip and then flowed toward the trailing edge with the cavity interface partially collapsing into small cavity bubble clusters. The rapidest collapsing and rebound were observed around the trailing edge from 0.7R to the tip during the final collapsing stages of the sheet cavitation. Immediately after the cavity collapsed, the intense flash from the collapsing cavity was found in the wide area from the tip towards the root.

(2) The blade surface cavitation on MP1-A and B (the moderately tip loaded propellers) extended to the relatively limited region around the tip and collapsed gradually, compared with that on MP1-D, i.e., lightly tip loaded one. The cavitation of MP1-A and B developed along the leading edge between 0.65R and 0.7R during its inception stage. The blade surface cavity grew and spread over the blade between 0.65 and 0.7R to the tip. The cavity collapsed near the trailing edge from 0.85 to the tip with slower speed than that in the lightly tip loaded case. The collapsing cavity was involved into the tip vortex cavitation and shed downstream.

(3) The blade surface cavitation on MP2-B to MP2-D (heavily tip loaded propellers) extended from 0.8R to the tip and confined to the relatively narrow region compared to those on blades of MPNo.1. The breakup of the cavity was delayed and the cavity shrank toward the tip smoothly.

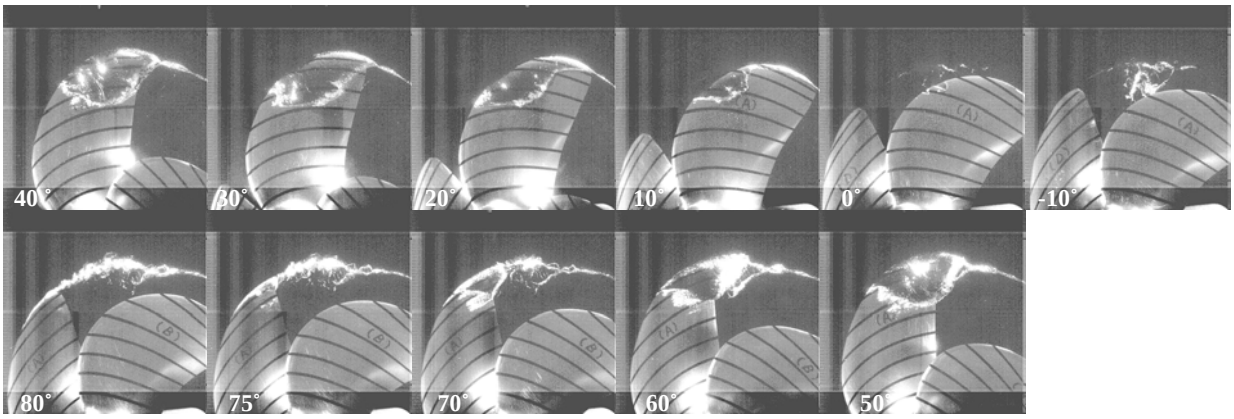

Figure 5 Cavitation of MP1-A

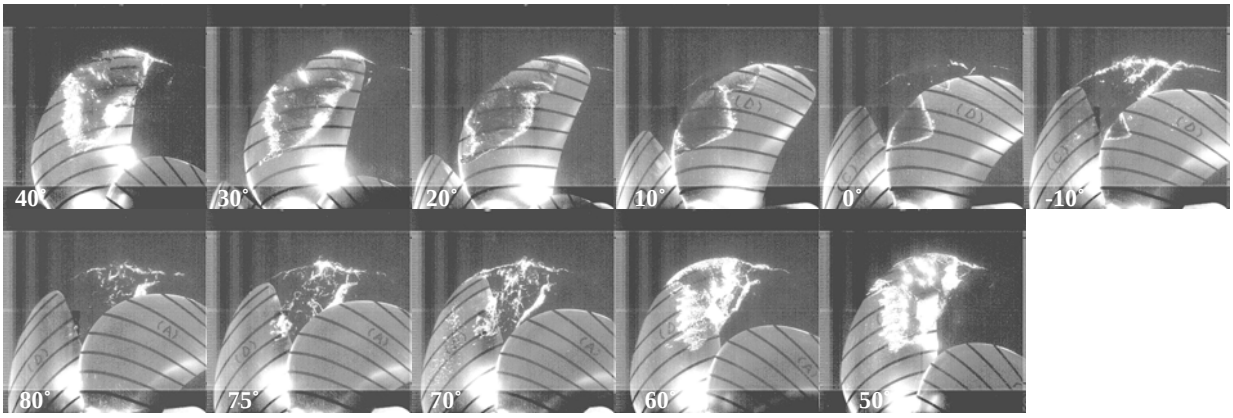

Figure 6 Cavitation of MP1-D

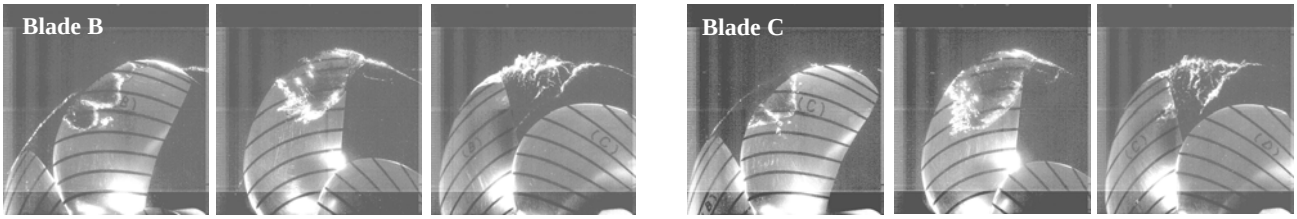

Figure 7 Cavitation of MP1-B and C

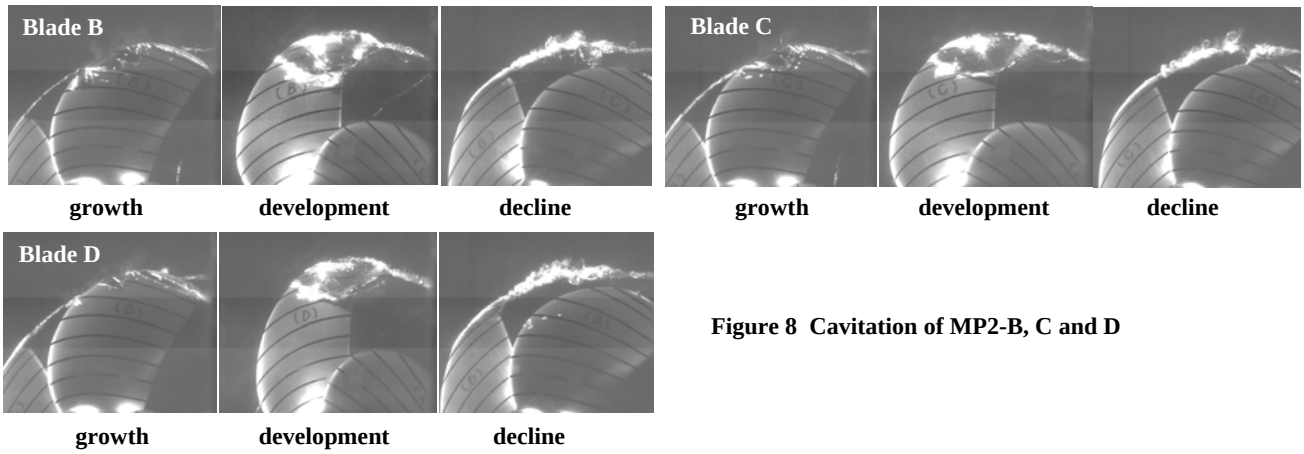

Figure 8 Cavitation of MP2-B, C and D

Figure 9 shows the state of blade surface of the suction side of MP1-A, B, C and D after the series of cavitation experiments. The blades of MP1-A and B had no damage and are expected to be used without serious risk of cavitation erosion. By contrast, the black lines drawn by a maker pen around the trailing edge at 0.9R and 0.95R of MP1-C was removed off. In the extreme case, such as MP1-D, the trailing edge at 0.95R chipped off and the lines at 0.9R and 0.95R were removed off. The trailing edge was slightly bent to the pressure side of the

trailing edge at 0.88R. No damage indicating erosion risk was found at the trailing edge between 0.7R and 0.8R where the rapid collapse of sheet cavity was observed. The blades of MP2-A, B, C and D were judged to have no risk of cavitation erosion. From the results of the present experiments, it is concluded that the sheet cavitation on the heavily tip loaded blades occurs limitedly around the tip and the cavity collapse is delayed until it is involved into the tip vortex cavitation. By contrast, the cavity on the lightly tip loaded blades tends to collapse on the blade surface and has more risk to cause cavitation erosion than that on the heavily tip loaded blades.

In order to examine the cavity behavior in detail, the variation of the cavity extent at each radial position was read from the sequential images taken by the high-speed video camera. Figure 10 shows the analyzed cavity extent of MP1-A reconstructed in this manner. In this figure, the abscissa indicates the angular position of the blade and 0 degrees mean the top position of the blade. The ordinate gives the chordwise position, where '0%' and '100%' mean the leading edge and the trailing edge of the blade respectively. The square and the circle symbols represent the leading edge and the trailing edge of the cavity. The sheet cavity exists in the region between the symbols.

The upward sloping straight line shows the positions of the cavity detachment from the leading edge of the blade at each angular position. The slope of this line indicates that the relative velocity of fluid particle making up cavity surface is the same as the circumferential velocity around the propeller blade. If the symbols move along this line, it means that the cavity locates at rest in space for the rotational direction of the propeller blade. From this figure, it can be found that after the cavity extended to a certain length, it detaches from the leading edge and flows toward the trailing edge nearly at the circumferential fluid velocity on the propeller blade surface with slightly decreasing its chordwise length.

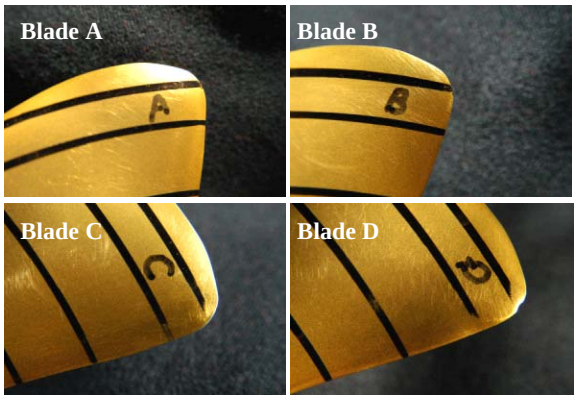

Figure 9 Cavitation erosion of MPNo.1

3.2 Measurement of Pressure Fluctuations

The measurement was carried out under the same experimental condition as that of the cavitation observation. Figure 11 shows the time history of fluctuating pressure signal measured on the flat plate with several pressure gauges immediately above a propeller. The characters of A, B, C and D in these figures correspond to the pressure signals induced by each blade A, B, C and D of MPNo.1 and 2 respectively. The peak to peak values of the wave pattern are shown in Table 4, comparing with the value of MPNo.0 as a score of 100. This value is proportional to the cavity extent. The peak to peak value of MP1-A is almost the same as that of MPNo.0. As the blade loads near the tip becomes heavier than that of MPNo.0, the pressure fluctuations induced by these blades slightly decrease. On the other hand, as the tip loads decrease, the pressure amplitudes remarkably increase. These results show that the heavily tip loaded propeller has an advantage over the lightly tip loaded propeller also on the pressure fluctuations.

4 CAVITATION SIMULATION

Numerical cavitation simulation was carried out by using the LST and the RANS to confirm the validity of these tools by comparing the computational results with the model test results described in the previous section.

4.1 Propeller Lifting Surface Theory

The unsteady lifting surface theory on the basis of the mode function method, e.g., (Hatano et al 1975) was used in the present numerical calculation.

Table 4 Fluctuating pressure (peak to peak)

PNo.	0	1	2	3	4	5	6	7
%	100	214	150	128	94	76	66	65

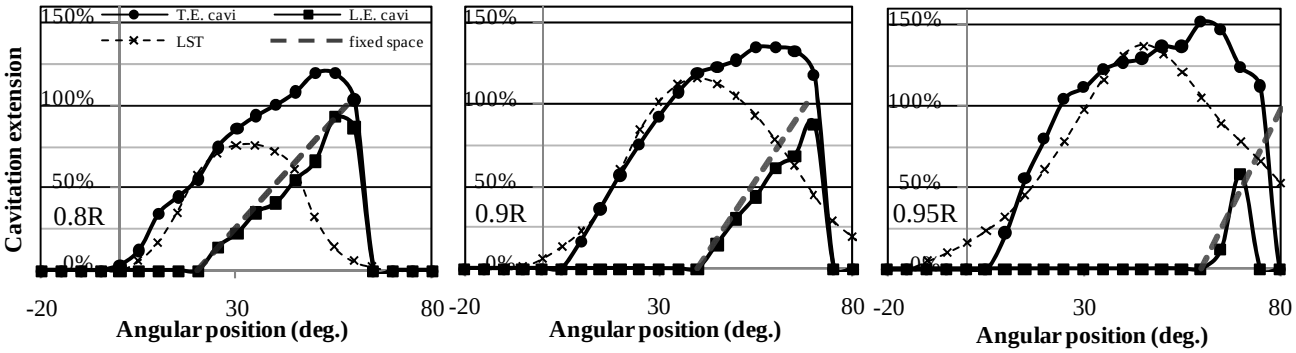

Figure 10 Cavitation extension of MP1-A

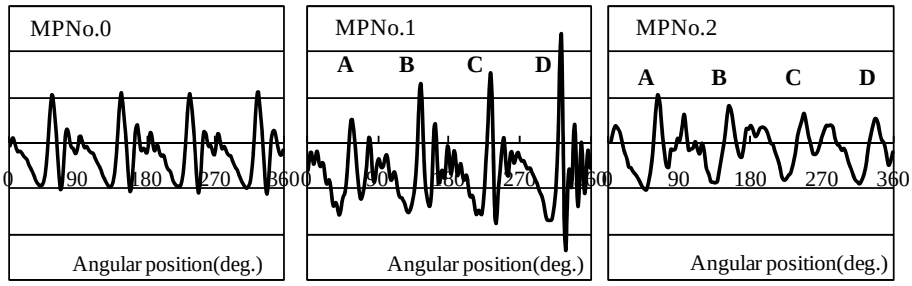

Figure 11 Wave pattern of fluctuating pressure

The hydrodynamically equivalent camber and equivalent attack angle, e.g., (Sugai 1971) were calculated from the circulation density distribution by the LST. The pressure distribution on the blade surface of the propeller working in the non-uniform hull wake in a quasi-steady manner was obtained by computing that on the equivalent two dimensional hydrofoil was calculated by the Moriya's conformal mapping method, e.g., (Moriya 1959), which is composed of the above equivalent camber and the geometric blade thickness distributions of the propeller, e.g., (Sugai 1971).

The criterion of cavitation inception and desinence is whether the blade surface pressure is higher or lower than the water vapor pressure and the extent of sheet cavity is calculated by the lift equivalent method, e.g., (Sugai 1971). It is well known that the phase angle of inception and desinence are different from the experimental results on a propeller working behind a wire mesh screen. Then, the present simulation predicts the phase angle delayed and the cavity extent from 0.9R to the tip longer than the original computations. The dotted lines in Figure 10 show the present simulation results on PNo.4. The predicted extent of cavity agrees well with the experimental results in the cavity developing stage, but it does not agree at all in the collapsing stage.

In the lower wake zone during one revolution of thepropeller blade, the load on the propeller blade and the back surface pressure becomes lower and higher than those in the higher wake zone respectively. Under such a condition, when the pressure on the blade becomes higher than the vapor pressure, cavitation should diminish. Although the present computation indicated that the pressure on the blade was higher than the vapor pressure, the cavity did not disappear and still existed on the blade in the observation. Taking these effects into consideration, the authors modified the criteria of cavitation simulation in the collapsing process, e.g., (Yamasaki et al 2008). The simulation results on PNo.1, 4 and 7 by the modified method are compared to the experimental results in Figure 12. The prediction of the cavity extent in the collapsing process around the trailing edge at the tip of each propeller was satisfactorily improved.

4.2 RANS

The authors have simulated the flow field around a propeller in both uniform and non-uniform wake using a commercial CFD code. In the present study, cavitation on MPNo.1 was simulated using SCRYU/Tetra V7 which is based on a finite volume method with an unstructured grid and supports various turbulence models. The Shear-

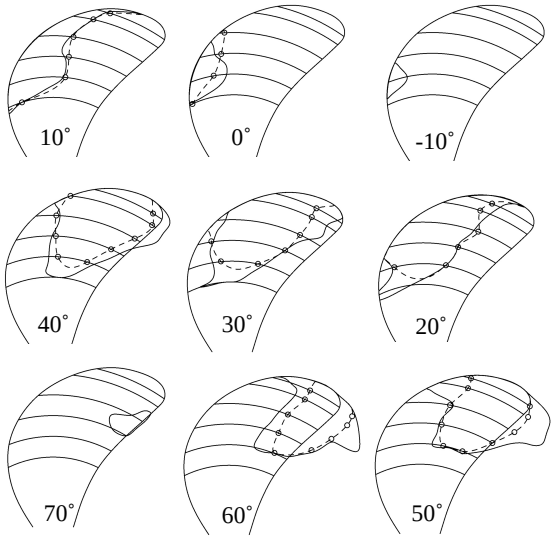

Figure 12a Estimated cavitation pattern of MP1-D (PNo.1) by LST(mod)

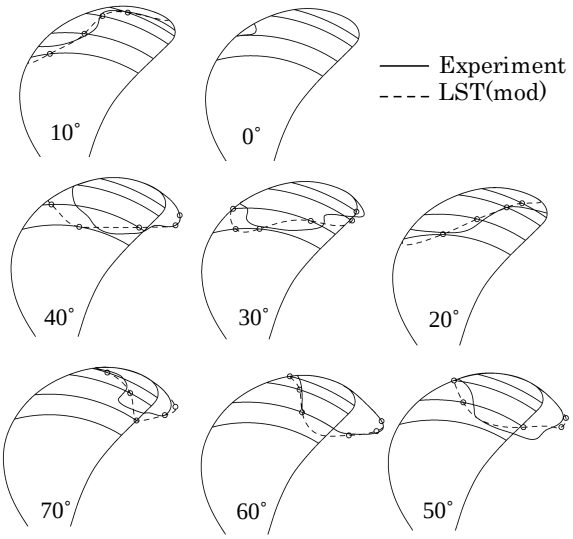

Figure 12b Estimated cavitation pattern of MP1-A (PNo.4) by LST(mod)

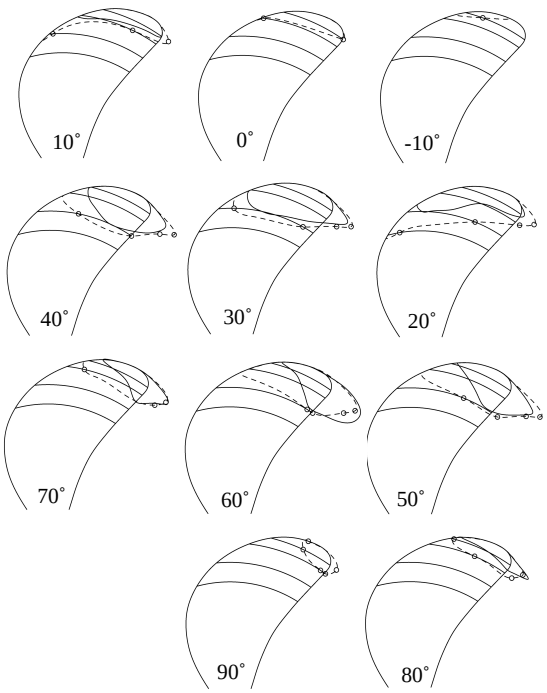

Figure 12c Estimated cavitation pattern of MP2-D (PNo.7) by LST(mod)

Stress Transport k-ω model was applied to the present simulations to compute the friction component of torque coefficient K_Q reasonably.

The computational domain was split into an outer stationary part and an inner rotating part including the propeller. The calculated propeller has different shapes of blades as the model of MPNo.1. Basic cells are tetrahedral and prismatic cells are applied to near the blade surface for resolving the boundary layer. Figure 13 shows the volume mesh region. Total number of elements for this volume is about 23 million.

The cavitation model used in this simulation is a barotropic model, e.g., (Okuda & Ikohagi 1996) included in SCRYU/Tetra V7. The equation of state for ideal gas and that for pure liquid proposed by Tammann were applied to the gas phase and to the liquid phase, respectively. This equation is approximated by a linear expression of temperature. P_C and T_0 are the pressure and temperature constants of liquid, and K is the liquid constant. These values are estimated by water property. R is the gas constant.

The gas-liquid two-phase medium inside the cavity is treated as a locally homogenous pseudo-single-phase medium with finite void ratio. The mixture density of a two-phase medium ρ is expressed by the linear combination with the local void fraction (volume fraction) of liquid phase density and gas-phase density with the assumption of a locally homogenous pseudo-single-phase medium. If the pressure P and temperature T of gas and liquid phase are in equilibrium, the equation of state for a locally homogenous pseudo-single-phase medium is given by using the mass fraction of gas phase Y in equation (1) as below.

$$\rho = \frac{P(P+P_c)}{K(1-Y)P(T+T_0)+R\,Y(P+P_c)T} \qquad (1)$$

As the inlet boundary condition, the void mass fraction was assumed to be 0.1%. Figure 14 shows the simulated results of cavitation extent. The boundary lines of cavitation correspond 0.5% of the void fraction over 0.2mm above the blade surface. The computed tip vortex became stronger with the increase of tip loading, namely in the order of MP1-D, C, B and A. These computational results reasonably correspond to the experimental results.

The extent of cavity became larger in the order of MP1-A, B, C and D, and the sheet cavity of MP1-A shrunk gradually toward the tip without violent collapse. The cavity of MP1-D was observed at the trailing edge like a patch. Such a cavity pattern suggests the risk of cavitation erosion. The RANS computations agree well with the experimental results qualitatively. But somehow the calculated void fraction is very low. Further study will be needed.

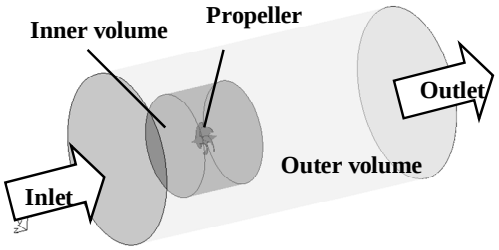

Figure 13 Volume mesh region

5 CONCLUSION

This paper has presented the remarkable effects of tip load distribution on cavitation performance of a propeller working in a non–uniform flow. Using two special propeller models with each blade systematically designed by different tip load distributions, experimental and numerical investigations were carried out in detail.

The following conclusion can be drawn,

(1) The cavitation experiment results show that the heavily tip loaded propellers give smaller cavitation extent restricted in the vicinity of the tip region and better performance against cavitation erosion and pressure fluctuations than the lightly tip loaded propellers, that is, the conventional tip unloaded one.

(2) The analysis of high speed video images taken in the cavitation observation demonstrates that the super-cavitated sheet cavity of the heavily tip loaded propellers diminishes more gradually and flows into tip vortex cavitation than the lightly tip loaded tip loaded propellers. This result suggests a possible cavitation control in the decline stage of sheet cavity in the design procedure.

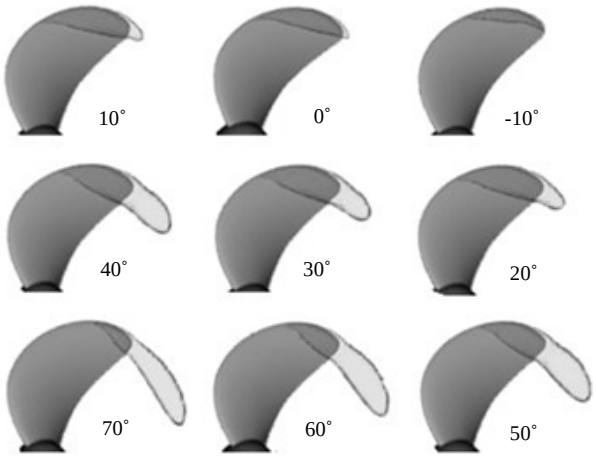

Figure 14a Estimated cavitation pattern of MP1-A by RANS

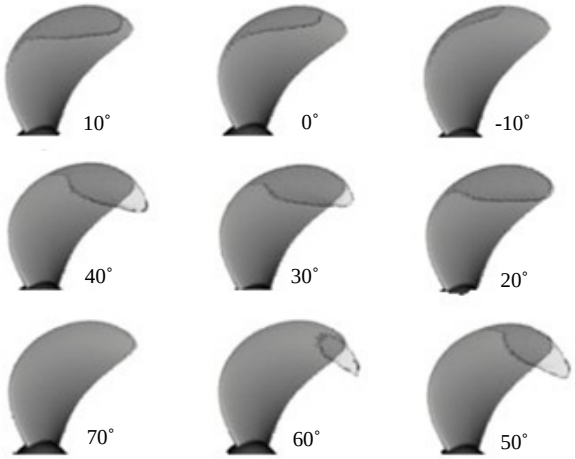

Figure 14b Estimated cavitation pattern of MP1-D by RANS

(3) From the comparison of two kinds of numerical simulation on cavitation behavior by a lifting surface theory and a RANS solver with the cavitation test results, the former predicts well the effect of tip load distribution on cavitation and the variation of cavitation extent including that in the cavity collapsing process at the tip by introducing the empirical correction factors based on the present experimental results. The latter also provides the qualitatively good agreement on cavitation extent and the effect of tip load distribution. Both methods are useful for design tools evaluating the risk of cavitation erosion.

In the cavitation test at IHI Corporation R&D Project Center, the authors are deeply grateful to Mr. M. Maruyama and Mr. H. Osaki of IHI Inspection & Instrumentation Co.,Ltd. for their generous support.

REFERENCES (* writen in Japanese)

Eckhardt, M. K. & Morgan, W.B. (1955). 'A Propeller Design Method'. Trans.SNAME. Vol. 63.

Hasuike, N., Yamasaki, S. & Ando, J.(2006). 'Prediction of Cavitation on Marine Propeller Using Generally Applicable Computation Fluid Dynamics', Proc. of 13th Symposium for Cavitation, Sapporo, Japan.*

Hasuike, N. & Yamasaki, S. (2006). 'Anti-Singing Edge Effect on Propeller Open Characteristics', SNAME Propellers and Shafting 2006, Virginia, U.S.A.

Hatano, S., Minakata, J. & Yamasaki, S.(1975). 'The Estimation of the Performance Characteristics of the Propeller by the Lifting Line and Lifting Surface Theory'. Trans. of The West-Japan Society of Naval Architects, No. 49, pp.177-220.*

Holden, K. & Kvinge, T., (1983), 'On Application of Skew Propellers to Increase Propulsion Efficiency', Proc. of 5th Lips Symposium, pp 4.3-4.19.

Johnsson, C.-A., (1981), 'Propeller Parameter Studies', Noise Sources in Ships: I Propellers, Nordforsk, Miljovardsserien, pp H1-H29.

Lerbs, H. W. (1952), 'Moderately Loaded Propellers with a Finite Number of Blades and Arbitrary Distribution of Circulation', Trans. SNAME, Vol.60, pp.73-117.

Moriya, T. (1959), 'Introduction to Aerodynamics', Tokyo, Baifukan.*

Okuda, K. & Ikohagi, T.(1996). 'Numerical Simulation of Collapsing Behavior of Bubble Clouds', Transactions of the Japan Society of Mechanical Engineers, B, vol.62, pp.3792-3797.*

Sugai, K. (1971), Proceedings of The 2nd Symposium on Marine Propellers, The Society of Naval Architects of Japan, Tokyo, Japan.*

Takahashi, H., (1959), 'A Prevention from Face Cavitation by Varying the Form of Blade Sections of a Screw Propeller', Report of Transportation Technical Research Institute, No. 38.

Ukon, Y. & Takei, Y., (1981), 'An Investigation of the Effects of Blade Profile on Cavitation Erosion of Marine Propellers', Trans. of the West-Japan Society of Naval Architects, No.61, pp.81-93.

Yamasaki, S. (1981), 'A Numerical Method for Non-Linear Steady Propeller Lifting Surface and Its Application for Highly Skewed Propeller Design'. Trans. of the West-Japan Society of Naval Architects, Vol. 62, pp. 47-68.*

Yamasaki, S. & Okazaki, A. 'Cavitation Test on a Straight Leading Edge Propeller and a Tip Rake Propeller'. Journal of the Japan Society of Naval Architects and Ocean Engineers, Vol. 2, pp. 271-277.*

Yamasaki, S., Okazaki, A., Ukon, Y. & Kawanami, Y. (2008) . 'Cavitation Test of a Propeller Having Blades Designed by Various Load Distributions near the Blade Tips 2nd Report : Modification of Cavitation Simulation by using Propeller Lifting Surface Calculation'. Proc. of Conference Proceedings the Japan Society of Naval Architects and Ocean Engineers, Vol. 6, pp. 201-204.*